NASA Technical Paper 2272

February 1984

Structural Efficiency Studies of Corrugated Compression Panels With Curved Caps and Beaded Webs

Randall C. Davis,
Charles T. Mills,
R. Prabhakaran,
and L. Robert Jackson

NASA

NASA
Technical
Paper
2272

1984

Structural Efficiency Studies
of Corrugated Compression Panels
With Curved Caps and Beaded Webs

Randall C. Davis
Langley Research Center
Hampton, Virginia

Charles T. Mills
and R. Prabhakaran
Old Dominion University
Norfolk, Virginia

L. Robert Jackson
Langley Research Center
Hampton, Virginia

INTRODUCTION

Efforts to improve performance for high-altitude high-speed aircraft and for spacecraft have motivated the search for minimum-mass fuselage and tank structures. The fuselage structures of such aircraft have external heat shields that provide an aerodynamically smooth surface. Thus, mass-efficient concepts which do not have a smooth outer surface can be used to carry the fuselage loads and to support the heat shields. An important limiting load in such aircraft is the compression buckling load of the fuselage wall, and a number of structural concepts have been investigated (ref. 1) for minimum mass under a compressive load. Of these concepts, the corrugated panel cross section (fig. 1) offers a very attractive mass-strength efficiency. Recent advances in the state of the art of superplastically forming and diffusion bonding (SPF/DB) technology (ref. 2) for a limited class of materials provide considerable freedom to design wall sections for high performance aircraft. In the present study, new structural concepts (figs. 1(b) through 1(d)) are proposed using the SPF/DB process that have a significant mass-saving potential over previous concepts for a wide range of loading.

The purpose of this paper is to report the results of a study of the structural efficiency of corrugated compression panels with curved caps and with beaded webs. In the study, the state-of-the-art optimization code PASCO (ref. 3) was used to mass-optimize these panels. Structural efficiency charts for the new concepts are presented, and various design features for making the panels mass efficient are discussed.

SYMBOLS

Values are given in both SI and U.S. Customary Units. Measurements were made in U.S. Customary Units.

A_{ij} laminate extensional stiffness matrix, N/m (lb/in.)

B_{ij} laminate coupling matrix, N/m (lb/in.)

b_f corrugation cap chord width, cm (in.)

b_w beaded-web pitch, cm (in.)

D_{ij} laminate bending stiffness matrix, N-m (lb-in.)

E isotropic elastic modulus, N/m^2 (psi)

E_{ij} elastic modulus, N/m^2 (psi)

G_{ij} shear modulus, N/m^2 (psi)

h filamentary composite lamina thickness, cm (in.)

h_w beaded-web depth, cm (in.)

k_4 edge support parameter; $3.29/(1 - \nu^2)$ for simply supported edges

L   panel length, cm (in.)

N   total number of laminae

N_x/EL panel compressive loading index

n   ratio of depth of cap curvature to cap thickness

Q_{ij} lamina stiffness modulus, N/m^2 (psi)

r_w beaded-web circular arc radius, cm (in.)

S_{ij} parameter defined by equation (A1)

t   thickness, cm (in.)

t_f corrugation cap thickness, cm (in.)

t_w beaded-web thickness, cm (in.)

$\bar{t}/L$ mass index

δ distance from reference to given lamina interface, cm (in.)

ε strain

θ angle of web to plane of panel, deg

θ_w beaded-web circular arc angle, deg

ν isotropic Poisson's ratio

ν_{ij} Poisson's ratio

STRUCTURAL CONFIGURATION

The basic function of the structurally efficient compression panel is to carry a design load over a distance without local buckling in the cross section and without buckling in a general or Euler instability mode. For Euler buckling strength, a structurally efficient panel cross section should have the load-carrying material symmetrically placed about the centroidal axis (ref. 4). Load-carrying material on or near the centroidal axis should be kept to a minimum since it contributes little to the overall cross-sectional bending stiffness and adds inefficient mass. In general, the corrugated-panel cross section (fig. 1) is a structurally efficient design because the load-carrying caps are symmetrically spaced about the panel centroidal axis by discrete webs. The most familiar structural corrugated panel cross section is the trapezoidal corrugation (fig. 1(a)) which has flat caps and flat webs. The webs in the trapezoidal corrugation, however, are load carrying. The proposed panel concepts shown in figures 1(b) through 1(d) offer an improvement in mass efficiency over the trapezoidal corrugation by reducing the load carried by the webs and by improving the local buckling strength of the caps.

Webs

Because the centroid of the web segment in a corrugation lies on the panel centroidal axis and contributes little to the overall bending stiffness, the amount of web material should be kept to a minimum. In the trapezoidal corrugation, the flat web must have at least the same local buckling strength as the flat cap. As a result, there is as much web material as there is cap material in the trapezoidal cross section. To improve local buckling strength, the web can be beaded in the direction perpendicular to the loading axis (figs. 1(b) through 1(d)). As a result, the web extensional stiffness in the load direction is drastically reduced, whereas its transverse bending stiffness is enhanced. The beaded web is non-load carrying and can be treated as a core material with an associated core density in the same manner as the honeycomb core in a sandwich structure. The depth of the beads gives the beaded web a substantial transverse bending stiffness and, thereby, allows the use of very thin gage web material. The beaded web provides a cross section with a substantial improvement in mass efficiency over the trapezoidal corrugation.

In earlier studies of beaded-web corrugated panels (ref. 1), the fabrication problem of attaching the beaded web to the cap was solved by tapering the depth of the web beads down to the thickness of a single sheet at the juncture with the caps. (See fig. 2(a).) For tapered beaded webs and thin gage web material, the single sheet of web material attached to the cap gives very little edge support to the cap, especially for buckling modes that involve twisting of the caps. As a result, the tapered beaded web requires a heavy gage web material to support the caps, which adversely affects the structural mass-strength efficiency. The SPF/DB process allows more freedom to design attachment of the beaded web to the caps without the necessity of tapering the beaded web down to the thickness of a single sheet. As can be seen in figure 2(b), with the SPF/DB process, the beaded web can be carried without taper to an intersection with the caps. The beaded-web intersection is spread out over an area as wide as or wider than the bead depth at the cap edge. With this method of attachment of web to cap, the full-depth beaded-web bending stiffness is used for stabilizing the edges of the caps against local buckling.

Caps

To improve local buckling strength, the caps of the corrugated panels are curved instead of flat. In the optimization process, the curvature has the effect of increasing the ratio of cap width to thickness over that of a flat cap at a given compressive load-strain level. An outward curvature in the caps, as shown in figure 1(b), adds to the structural efficiency by moving the centroid of the load-carrying cap material to a more efficient position away from the panel centroidal axis compared with the flat cap without increasing the length of the webs.

In the interest of giving the curved-cap corrugated panel some resistance to dimpling, the curvature of the caps may be reversed or inverted as shown in figure 1(c). In this configuration, a foreign-object impact spanning several corrugations of the panel would presumably occur at the edges of the caps rather than at the center of the caps. An additional feature that may be incorporated to improve the cap local buckling strength is to extend the width of the cap and crimp the edges down a short distance over the beaded webs as shown in figure 1(d). This feature insures a straight edge for the cap and, if the crimped edges are bonded at each discrete crest of the web beads, a stiffer edge support for the cap.

Filamentary Composite Corrugation

The primary mass-saving potential achieved with filamentary composites comes from using low density materials. However, an investigation was made of the mass-saving potential added to a filamentary composite corrugation by curved caps stabilized by deep webs (fig. 3). Filamentary composite fabrication processes do not lend themselves to making beaded webs. To achieve the needed web depth for local buckling strength and for stabilizing the edges of the caps, the corrugation construction considered has a web with a low density foam insert and encapsulating outer plies. To reduce the load-carrying stiffness of the web, the layers encapsulating the foam insert were cross plied. For the curved-cap filamentary composite corrugation studied in this report, it was assumed, for manufacturing reasons, that the cross-ply layers are four continuous $\pm45°$ plies throughout the corrugated panel cross section and thereby encapsulate the foam inserts as well as the unidirectional load-carrying zero-degree filament layers used for selective stiffening in the caps. The thickness of the foam insert was arbitrarily chosen to be equal to the thickness of the zero-degree cap plies.

Geometric Parameters

In the analysis of the curved-cap corrugated panel, the notation shown in figure 4(a) is used. The depth of the curvature in the caps is expressed as a multiple n of the cap thickness t_f. The depth nt_f is measured from the cap midsurface at midspan to the chord between the cap edges. To analyze the curved caps with the PASCO code, the cap was broken into five equal-length straight segments. The five segments were then used to approximate the circular arc. The angle between each straight segment centerline and the chord of the circular arc was computed by using an initial guess for nt_f. A preliminary PASCO analysis was made to obtain an optimum cross section and a value for cap thickness. The angles for each straight segment were then recomputed for reoptimization in PASCO so that all the corrugations would have nearly the same value for n. For this report, the value of n for the entire range of loading was kept between 4 and 6 for all the corrugations studied.

The cross section of the beaded web shown in figure 4(b) is determined by specifying the web thickness t_w, bead spacing b_w, and bead depth h_w. Beaded-web shapes can be sinusoidal, circular, or any other suitable shape. In this report, the circular arc was arbitrarily chosen as the web shape for the SPF/DB metallic corrugations. To input the beaded-web section properties into the corrugation cross-sectional model in PASCO, the properties of the web had to be transformed to an equivalent layered segment. A model of the beaded-web cross-sectional geometry shown in figure 3(b) was made and a PASCO analysis of the model was used to compute extensional and bending stiffness values. These stiffness values were rotated through 90° and subsequently converted, by the method given in the appendix, to equivalent lamina properties for use in PASCO. Since PASCO input is specifically designed for layered input, individual layer properties for the filamentary composite corrugations could be input directly into PASCO.

RESULTS AND DISCUSSION

Various beaded-web geometries were investigated for the SPF/DB metallic corrugations in this study. Analytical results using these geometries, as well as manufacturing considerations, led to the selection of the beaded-web geometry shown in figure 4(b), which was used for the entire load ranges considered in this report. The

4

minimum gage web thickness thought to be feasible from superplastically forming was 0.0127 cm (0.005 in.). The value of θ for the angle between the web and the plane of the panel used in this report was found from the PASCO analyses to be nearly optimum at 60° over a wide range of the loading index.

Cap-to-Web Junction

In the flat-cap corrugated panel of reference 1, the beaded-web geometry tapered to the thickness of a single sheet at the junction with the cap. The beaded-web attachment, however, was assumed to be sufficient to provide a simple support edge condition for the cap. It was noted in reference 1 that the assumption of simply supported cap edges should be verified by test.

An attempt was made in this study to supply some of the edge support verification sought in reference 1 by a PASCO analysis of a detailed model of the tapered beaded web. In the PASCO model of this corrugation, the smooth web taper was approximated by three equal-length web sections that changed from the full-depth beaded-web section to the thickness of a single sheet in three steps. For computing section properties, the cross section of each step was circular as shown in figure 4(b), except that the angle θ_w was decreased in each step. For the first tapering step, the angle θ_w was decreased so that the beaded-web height was two-thirds the full depth given in figure 4(b). Similarly, for the second tapering step, the angle θ_w was decreased so that the height was one-third the full depth. The final and third tapering step was an unbeaded flat sheet with a thickness of t_w. Each step had the same length arbitrarily chosen to be equal to the beaded-web full depth.

The structural efficiency results for the tapered-web model are shown in figure 5 and compared with the results obtained for a flat-cap corrugation with webs that did not taper. Figure 5 shows the variation of the mass index $\bar{t}/L$ with the strength index N_x/EL. (Mass-strength indices were proposed by Shanley (ref. 4) for comparing panel constructions.) Use of the dimensionless indices $\bar{t}/L$ and N_x/EL removes the effect of material properties from the efficiency curves and permits a comparison of structural efficiencies on the basis of cross section alone. The $\bar{t}$ used in $\bar{t}/L$ is a mass-equivalent thickness for the corrugated cross section. Multiplying $\bar{t}/L$ by the material density gives the panel mass per unit area per unit length. The analytical results show that the tapered webs at moderate to heavy loading levels supply a nearly simple support condition to the cap edges; thereby, the local buckling loads in the caps are in line with the results in reference 1. This support, however, is not sufficient to prevent buckling modes involving twisting of the caps. These modes could not be determined in the optimization techniques used in reference 1. These modes, accounted for in PASCO, occur at load levels lower than those given by the simply supported plate buckling modes assumed in the caps in reference 1. The tapering of the webs to the thickness of a single web sheet results in a corrugation about 6 percent less efficient than a flat-cap full-depth beaded-web structure as can be seen in figure 5. These results also show that a wide variation in the support condition for the edges of the cap has only a small effect on the structural efficiency. Therefore, the simple support edge condition assumed in reference 1 for the caps was a reasonable assumption.

A study of the PASCO results for the beaded-web corrugated panels revealed that the fixity condition for the cap edges varied from nearly simply supported to nearly clamped. The corresponding values of edge support parameter k_4 varied from 3.6 to 6.3. This wide variation in edge condition is attributed to the fact that the cap thickness varied with load level, whereas the beaded-web geometry was held constant.

At low load intensities, the cap thickness approached minimum gage, and the cap transverse bending stiffness became significantly smaller (of the order of 1/10) than the transverse bending stiffness of the beaded web. Thus at low loading levels, the beaded web gives a nearly clamped support condition to the caps. At higher loading intensities, the cap thickness increased and the cap transverse bending stiffness became greater (of the order of 10) than the transverse bending stiffness of the beaded web. Thus at high loading levels, the beaded web gives a nearly simple support condition to the cap edges. These results suggest that the web chosen for this study provides adequate support to the caps (k_4 of about 4.3) over a wide range at the middle loading levels, but the support should be improved for the higher loading levels. It would seem from this study that the most appropriate choice of beaded-web shapes would be a web geometry that had a transverse bending stiffness of the same order as the cap transverse bending stiffness at all load levels. If this condition is met, then k_4 varies only slightly about an average value of about 4.3.

<div align="center">Flat Webs and Beaded Webs</div>

The mass-strength results from an optimized PASCO model of the trapezoidal corrugation with flat caps and flat webs are shown in figure 6. As shown, the curved-cap beaded-web corrugation offers an improvement in mass-saving potential of up to 50 percent better than the trapezoidal corrugation. Most of this large improvement in structural efficiency is a direct result of beading the webs which allows the web to be made of a much thinner material than the caps. The centroid of a corrugation web lies in an inefficient position on the neutral axis of the panel. To achieve sufficient panel bending stiffness for Euler buckling strength, the load-carrying flat web of the trapezoidal corrugation must have a ratio of thickness to width the same as that for the caps to resist local buckling. For the trapezoidal corrugation shown in figure 6, the web and cap thicknesses are equal. If the web is beaded, it is no longer load carrying and, therefore, can be made of a very thin gage material. The loss in panel stiffness from beading the webs is made up by more material in the caps which are located in a more efficient position away from the neutral axis of the panel. Since the beaded-web material is non-load carrying, its mass can be treated as a core material in much the same way as the honeycomb core in a sandwich structure. Resulting mass indices for the beaded-web corrugation are about 80 percent of the mass indices for the 1-percent honeycomb wide column that is used in the figures as a standard of comparison in this report.

<div align="center">Curved Caps</div>

The mass-strength optimization results from PASCO for corrugated panels with full-depth beaded webs and flat caps are also compared in figure 6 with the results for a corrugation with full-depth beaded webs and curved caps. From the curved panel buckling formula (ref. 5), it can be seen that the addition of a small amount of curvature in the caps of the corrugated panel greatly enhances the local buckling strain in the caps (fig. 7). A study of all the results from the mass-strength analyses of the corrugations revealed that the increase in the mass-saving advantage from increased amounts of cap curvature became negligibly small for curvatures with values of n greater than about 6. The predominant effect on efficiency of adding curvature to the caps is that an increase in cap width is achieved over a flat cap for a given compressive load-strain level (fig. 7). With wider caps, the non-load-carrying beaded-web material is spaced farther apart in the curved-cap corrugation than in a flat-cap corrugation. The curved-cap corrugation core material becomes a smaller portion of the panel mass compared with the flat-cap corrugation and gives a

6

lower core density ratio for the curved-cap beaded-web corrugated panel. As a result, the optimization curves in figure 6 for the curved-cap concept show a 12-percent mass-reduction potential over the corrugation with flat caps in the buckling limited range of the load index.

The mass-strength efficiency curve for a corrugated panel with inverted caps is compared in figure 8 with the curved-cap beaded-web corrugation efficiency curve. As can be seen, the mass penalty for inverting the caps is of the order of 6 to 7 percent. The inverted-cap beaded-web corrugation, however, still has a mass-saving potential that is about 6 percent better than the flat-cap beaded-web corrugation.

Crimping the edges of the caps is a practical fabrication technique for preserving a straight cap edge. In addition, crimping the edges should strengthen the caps against impact damage and improve the local buckling strength of the corrugated panel caps. The mass penalty for adding a 0.254-cm (0.1-in.) crimp to the edge of the inverted caps can be seen in the results shown in figure 9. The mass penalty for crimping the edges was found to be about a 4-percent mass increase compared with the inverted curved-cap beaded-web corrugation without crimped edges.

Filamentary Composite Panels

The mass-saving advantage of adding curvature to the caps of a filamentary composite corrugated panel can be seen from the results shown in figure 10. The optimized mass-strength efficiency curve for the composite corrugation with curved and flat caps and foam inserts in the webs is compared with the efficiency curve for an optimized flat-cap corrugation with no foam insert in the webs. It was assumed that the bond between the foam insert and the cross plies is sufficient to prevent wrinkling of the composite layers. As can be seen in figure 10, the addition of cap curvature and foam inserts improves the mass-strength efficiency by 35 to 40 percent over that of the flat-cap corrugation with no foam inserts. Comparing the efficiency curves for the foam insert corrugations with flat and curved caps shows that the cap curvature improves the efficiency by about 12 percent. Note that the composite structure efficiency curve is above the 1-percent honeycomb efficiency curve, whereas in previous figures the metallic beaded-web curved-cap corrugation was below that of the 1-percent honeycomb. The composite corrugation structure studied does not utilize its load-carrying material as efficiently as the metallic beaded-web corrugation. However, the lower material density offered by composite materials is more than enough to give panel structures with lower mass per unit panel area per unit length than the metallic beaded-web corrugations. The advantages of both metallic beaded webs and filamentary composites could be combined by using an SPF metal corrugation selectively reinforced with bonded composite caps. Such a configuration should be the object of another study.

CONCLUDING REMARKS

The combination of curved caps and beaded webs in corrugated compression panels produces mass-strength efficiencies that are better than that of a 1-percent core honeycomb structure. The mass-strength efficiency of the beaded-web curved-cap concept offers a potential 50-percent mass saving over conventional panels with flat caps and flat webs.

The addition of a small amount of curvature to the caps of a corrugated panel enhances the local buckling strength of the caps. In addition, for a given

load-strain level, a wider cap width is possible which means a wider web spacing is achieved for the curved cap than for a flat cap. As a result, the optimization curve shows a potential 12-percent mass reduction for the curved-cap concept compared with the flat-cap corrugation in the buckling limited range of load index.

Beading the webs of corrugated panels increases their transverse bending stiffness. The webs can then be made of very thin gage materials without incurring loss of local buckling strength under load. Since the beaded web is non-load carrying, the web material may be considered as a core material in much the same way as the honeycomb core in a sandwich structure. Resulting mass indices are about 80 percent of the mass indices for a 1-percent honeycomb wide column.

Corrugated panels with caps that are curved inward or inverted to improve damage tolerance are only about 6 to 7 percent less mass efficient than corrugated panels with outward cap curvature. Adding crimped edges to ensure straight cap edges and to improve damage tolerance as well as improve local buckling strength in the caps increases the mass about 4 percent compared with that of the plain edge curved-cap corrugated panel.

For the filamentary composite corrugation, adding curvature to the caps and using foam inserts to increase the thickness of the web improve mass efficiency by about 35 percent over a flat-cap, no-foam-insert filamentary composite corrugated panel. The buckling strain of the load-carrying web, however, is still governed primarily by the geometric ratio of web thickness to web width; hence, the mass-reduction potential achieved by beading the webs cannot be achieved with the filamentary composite concept studied in this report. A more efficient approach would be to use a beaded-web metallic corrugation as a core and then bond filamentary composites to the caps for selective strengthening of the hybrid composite corrugation.

Langley Research Center
National Aeronautics and Space Administration
Hampton, VA 23665
January 26, 1984

APPENDIX

REDUCTION OF GENERAL CROSS-SECTIONAL PROPERTIES
TO THREE EQUIVALENT LAYERS

The stiffnesses of an N-layer laminate, such as shown in figure 11(a), are given by the expression

$$(S_{ij})_m = \frac{1}{m} \sum_{k=1}^{N} (Q_{ij})_k (h_k^m - h_{k-1}^m) \qquad (m = 1, 2, \text{ and } 3) \qquad \text{(A1)}$$

where the values of $(Q_{ij})_k$ are generalized lamina stiffnesses. (See ref. 6.) The extensional stiffness matrix A_{ij} is given by

$$A_{ij} = (S_{ij})_1 \qquad \text{(A2)}$$

the coupling matrix B_{ij} is given by

$$B_{ij} = (S_{ij})_2 \qquad \text{(A3)}$$

and the bending stiffness matrix is given by

$$D_{ij} = (S_{ij})_3 \qquad \text{(A4)}$$

Equation (A1) gives, for a laminate with any number of laminae, S_{ij} in terms of $(Q_{ij})_k$. Suppose S_{ij} for the laminate is known, then the three expressions from equation (A1) can be solved for three values of $(Q_{ij})_k$ for three equivalent layers in terms of the known S_{ij}. The resulting solution, using the notation shown in figure 11(b), is

$$(Q_{ij})_1 = \left[\frac{\delta_1\delta_2 + \delta_2\delta_3 + \delta_1\delta_3}{(\delta_1 - \delta_0)(\delta_2 - \delta_0)(\delta_3 - \delta_0)} A_{ij} - \frac{2(\delta_1 + \delta_2 + \delta_3)}{(\delta_1 - \delta_0)(\delta_2 - \delta_0)(\delta_3 - \delta_0)} B_{ij} + \frac{3}{(\delta_1 - \delta_0)(\delta_2 - \delta_0)(\delta_3 - \delta_0)} \right] D_{ij}$$

$$(Q_{ij})_2 = \left[\frac{(\delta_2 - \delta_0)(\delta_3 - \delta_0)(\delta_3 - \delta_1) - (\delta_1\delta_2 + \delta_2\delta_3 + \delta_1\delta_3)(\delta_3 - \delta_1) - (\delta_2\delta_0 + \delta_1\delta_0 + \delta_1\delta_2)(\delta_2 - \delta_0)}{(\delta_2 - \delta_1)(\delta_3 - \delta_1)(\delta_2 - \delta_0)(\delta_3 - \delta_0)} \right] A_{ij}$$

$$+ 2 \left[\frac{(\delta_1 + \delta_2 + \delta_3)(\delta_3 - \delta_1) + (\delta_0 + \delta_1 + \delta_2)(\delta_2 - \delta_0)}{(\delta_2 - \delta_1)(\delta_3 - \delta_1)(\delta_2 - \delta_0)(\delta_3 - \delta_0)} \right] B_{ij} - 3 \left[\frac{(\delta_3 - \delta_1) + (\delta_2 - \delta_0)}{(\delta_2 - \delta_1)(\delta_3 - \delta_1)(\delta_2 - \delta_0)(\delta_3 - \delta_0)} \right] D_{ij}$$

$$(Q_{ij})_3 = \left[\frac{\delta_2\delta_0 + \delta_1\delta_0 + \delta_1\delta_2}{(\delta_3 - \delta_2)(\delta_3 - \delta_1)(\delta_3 - \delta_0)} \right] A_{ij} - \left[\frac{2(\delta_0 + \delta_1 + \delta_2)}{(\delta_3 - \delta_2)(\delta_3 - \delta_1)(\delta_3 - \delta_0)} \right] B_{ij} + \left[\frac{3}{(\delta_3 - \delta_2)(\delta_3 - \delta_1)(\delta_3 - \delta_0)} \right] D_{ij}$$

$$\left. \right\} \qquad \text{(A5)}$$

The values of δ_k are arbitrarily chosen and the resulting values of $(Q_{ij})_k$ are independent of the reference surface used. Thus for any given set of equivalent laminate thicknesses $(\delta_k - \delta_{k-1})$, equivalent values of $(E_{ij})_k$ computed from the resulting values of $(Q_{ij})_k$ are unchanged by changes in δ_0. Therefore, for convenience of computing the equivalent moduli, the reference surface can be chosen as the midsurface.

Equations (A5) are only of general interest and are now put into a more practical form for analyzing the beaded web of a corrugation for PASCO. The equivalent layers may all be chosen to be the same thickness h, in which case, the equations for $(Q_{ij})_k$ reduce to the simpler form

$$\left. \begin{aligned} (Q_{ij})_1 &= \frac{1}{2}\left(-\frac{1}{12h}A_{ij} - \frac{1}{h^2}B_{ij} + \frac{1}{h^3}D_{ij}\right) \\[2mm] (Q_{ij})_2 &= \frac{13}{12h}A_{ij} - \frac{1}{h^3}D_{ij} \\[2mm] (Q_{ij})_3 &= \frac{1}{2}\left(-\frac{1}{12h}A_{ij} - \frac{1}{h^2}B_{ij} + \frac{1}{h^3}D_{ij}\right) \end{aligned} \right\} \tag{A6}$$

With the values of Q_{ij} known, the equivalent E_{ij} for each layer is determined from

$$\left. \begin{aligned} Q_{11} &= \frac{E_{11}}{1 - \nu_{12}\nu_{21}} \\[3mm] Q_{22} &= \frac{E_{22}}{1 - \nu_{12}\nu_{21}} \\[3mm] Q_{12} &= \frac{\nu_{21}E_{11}}{1 - \nu_{12}\nu_{21}} = \frac{\nu_{12}E_{22}}{1 - \nu_{12}\nu_{21}} \\[3mm] Q_{66} &= G_{12} \\[3mm] Q_{16} &= Q_{26} = 0 \end{aligned} \right\} \tag{A7}$$

The $(E_{ij})_k$ equivalent properties computed with Q_{ij} from equations (A6) are unchanged by changes in h. Thus, ply thickness changes can be made easily without recomputing $(Q_{ij})_k$. A summation of the relations (A6) produces the check that the sum of $(Q_{ij})_k$ equals A_{ij}/h. If the values of B_{ij} are all zero, then from the special reduced relations (eqs. (A6)) the outer two layers (1 and 3) have the same elastic properties.

The equivalent three-layer laminate with these equivalent $(E_{ij})_k$ values reproduces the A_{ij}, B_{ij}, and D_{ij} matrices for any type of thin structure, except that the anisotropic terms (16 and 26 terms) in the A_{ij}, B_{ij}, and D_{ij} matrices for the

three-layer equivalent laminate are zero. Conversely, the values of $(E_{ij})_k$ are unaffected if the anisotropic terms in the A_{ij}, B_{ij}, and D_{ij} matrices are ignored in computing $(E_{ij})_k$. Thus, the A_{ij} and D_{ij} matrices generated for a model of the beaded web can be input to PASCO through a three-layer equivalent laminate without loss in the essential structural properties of the beaded web.

REFERENCES

1. Giles, Gary L.: Structural Efficiencies of Five Compression Panels With Curved Elements. NASA TN D-6479, 1971.

2. Bales, Thomas T., ed.: SPF/DB Titanium Technology. NASA CP-2160, October 1980.

3. Anderson, Melvin S.; and Stroud, W. Jefferson: A General Panel Sizing Computer Code and Its Application to Composite Structural Panels. AIAA J., vol. 17, no. 8, Aug. 1979, pp. 892-897.

4. Shanley, F. R.: Weight-Strength Analysis of Aircraft Structures, Second ed. Dover Publ., Inc., c.1960.

5. Roark, Raymond J.; and Young, Warren C.: Formulas for Stress and Strain, Fifth ed. McGraw-Hill, Inc., c.1975.

6. Ashton, J. E.; Halpin, J. C.; and Petit, P. H.: Primer on Composite Materials: Analysis. Technomic Pub. Co., Inc., c.1969.
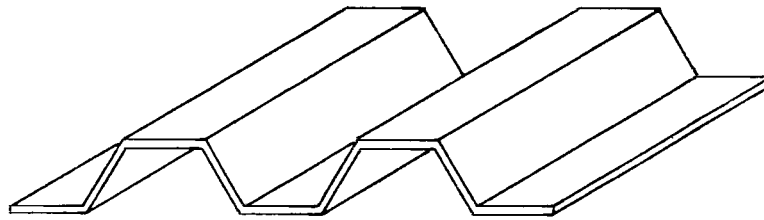
(a) Trapezoidal corrugation.
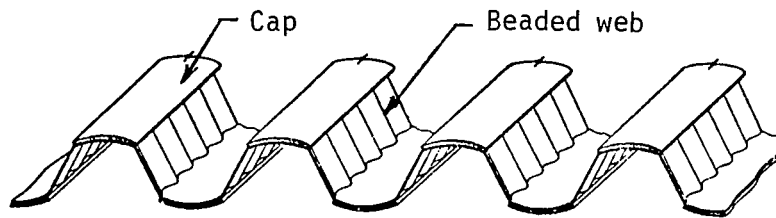
(b) Curved-cap beaded-web corrugation.
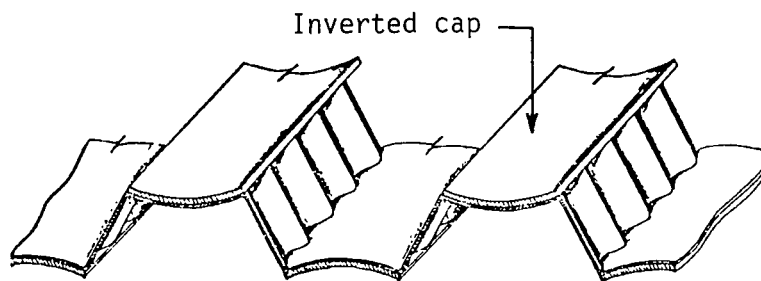
(c) Inverted-cap beaded-web corrugation.
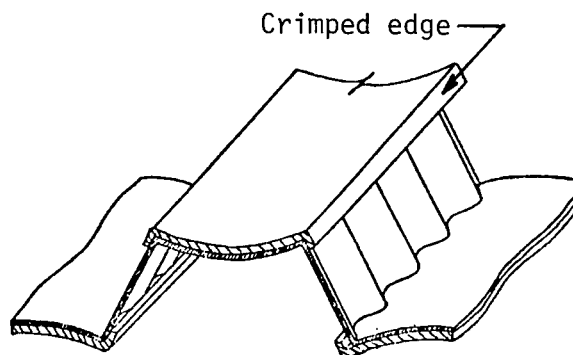
(d) Crimped-edge cap corrugation.

Figure 1.- Geometric configurations for corrugated panels.

Cap width

Cap

Cap
thickness

Beaded web

A

B

A

B

Section A-A
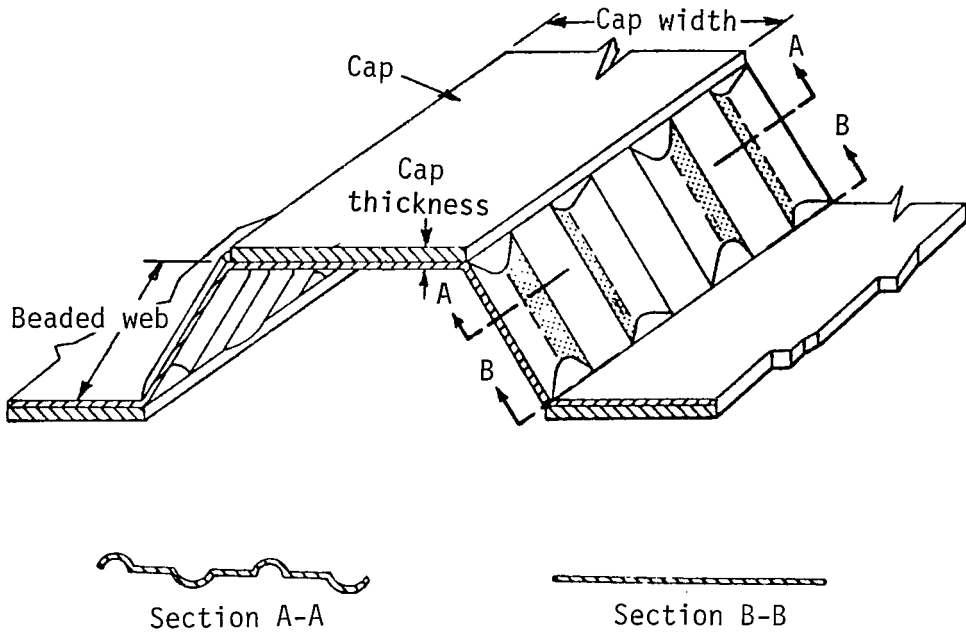
Section B-B

(a) Corrugated panel with tapered beaded web.

Cap

Section B-B

Section A-A

Cap

A

B

B

A
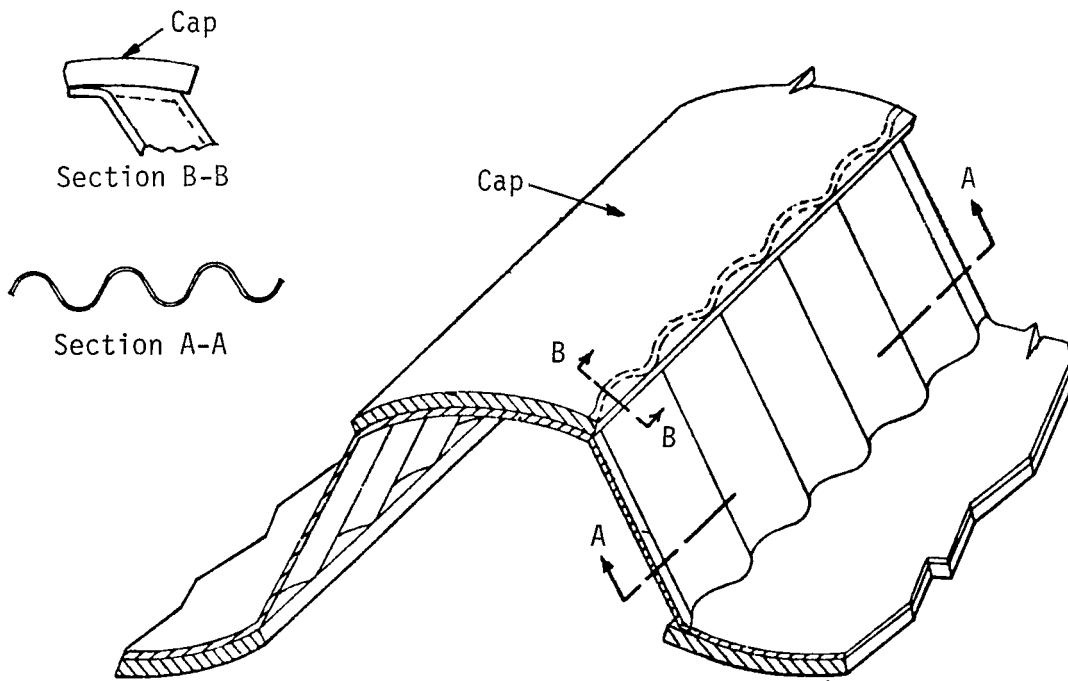
(b) Corrugated panel with nontapered beaded web.

Figure 2.- Corrugated panel cross-section detailing attachment of
beaded webs to caps.
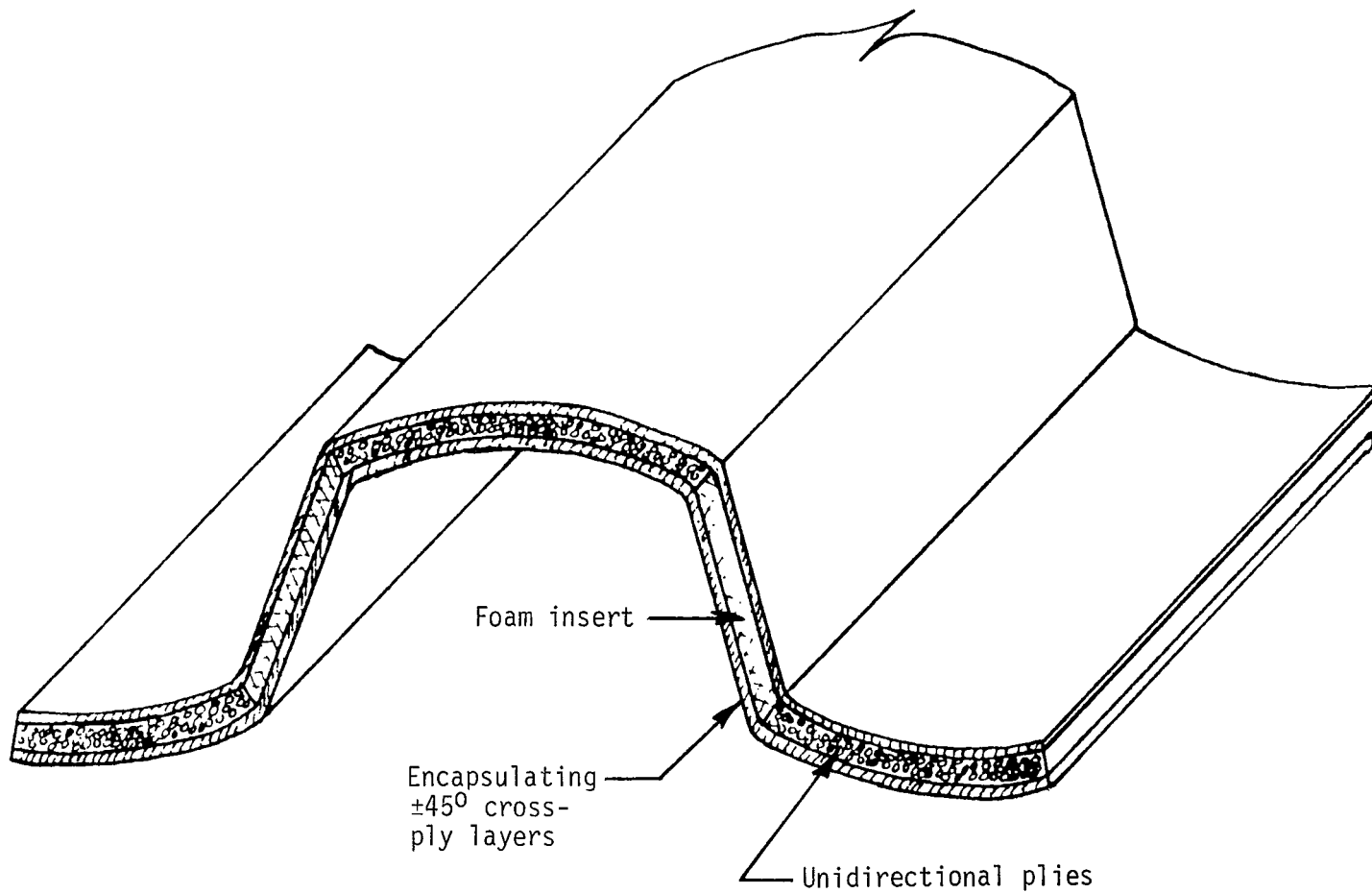
Figure 3.- Curved-cap composite corrugation concept.

Foam insert

Encapsulating ±45° cross-ply layers

Unidirectional plies
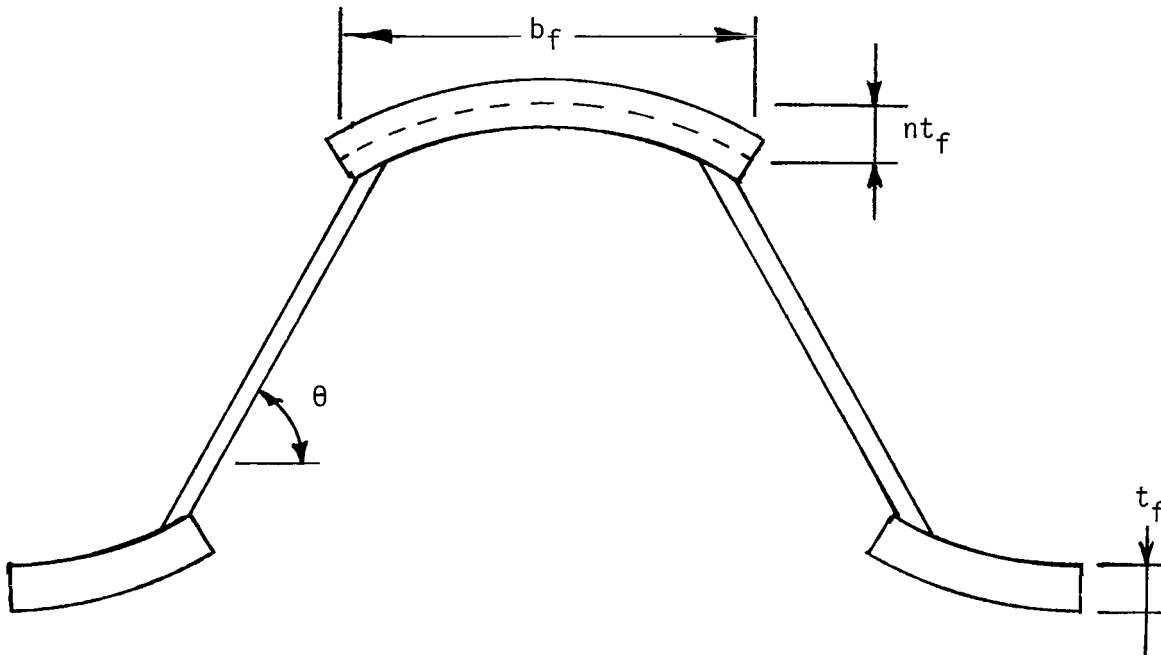
(a) Curved-cap corrugation geometry.
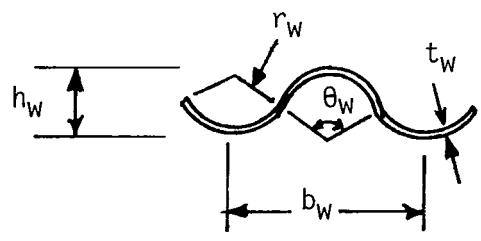
h_w = 0.318 cm (0.125 in.)
b_w = 0.952 cm (0.375 in.)
t_w = 0.0127 cm (0.005 in.)
r_w = 0.259 cm (0.102 in.)
θ_w = 135°

(b) Beaded-web geometry.

Figure 4.- Schematic of curved-cap beaded-web corrugation defining nomenclature for cross section.
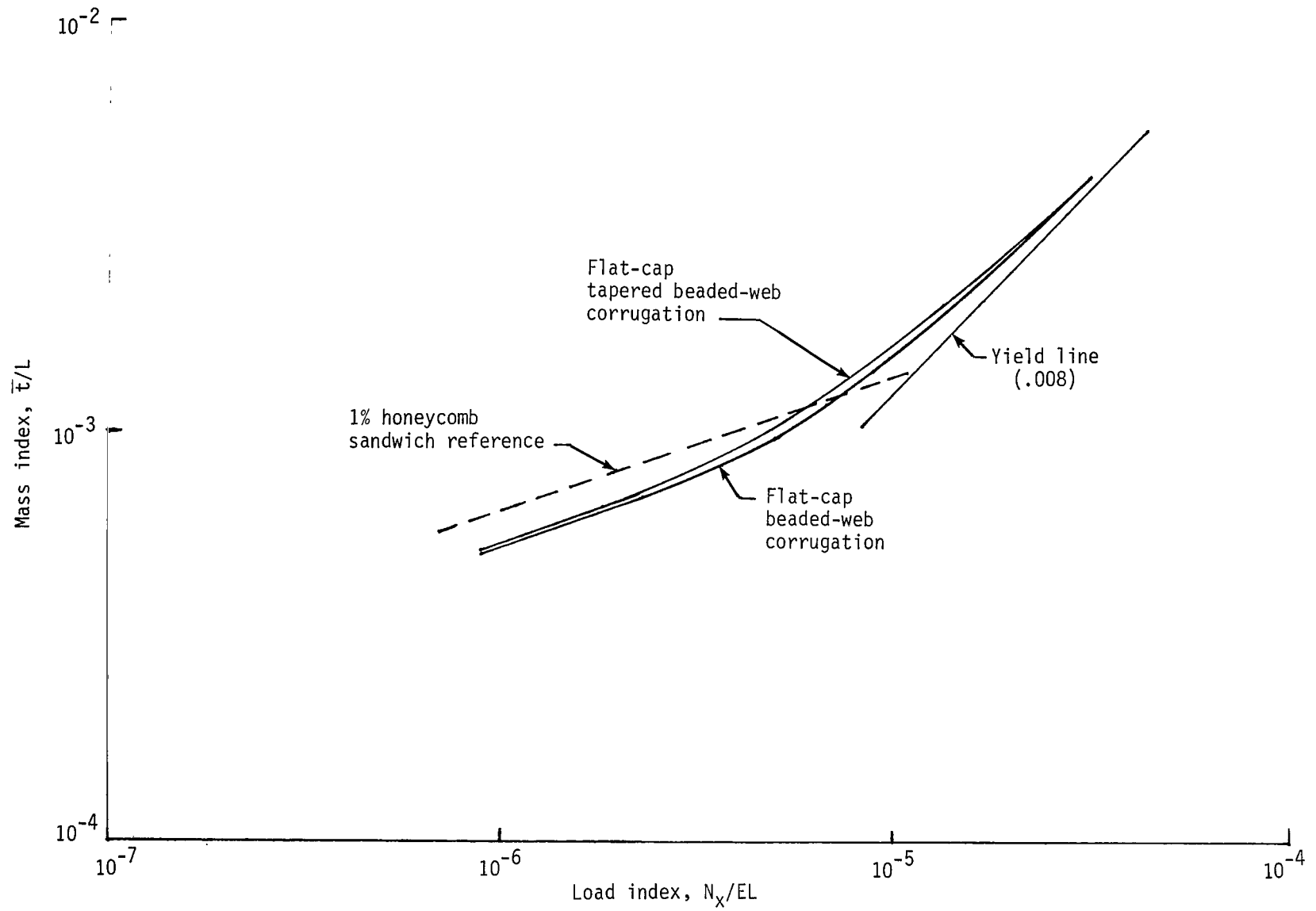
Figure 5.- Comparison of flat-cap corrugations showing effect on structural efficiency of tapering beaded web at junction with cap.
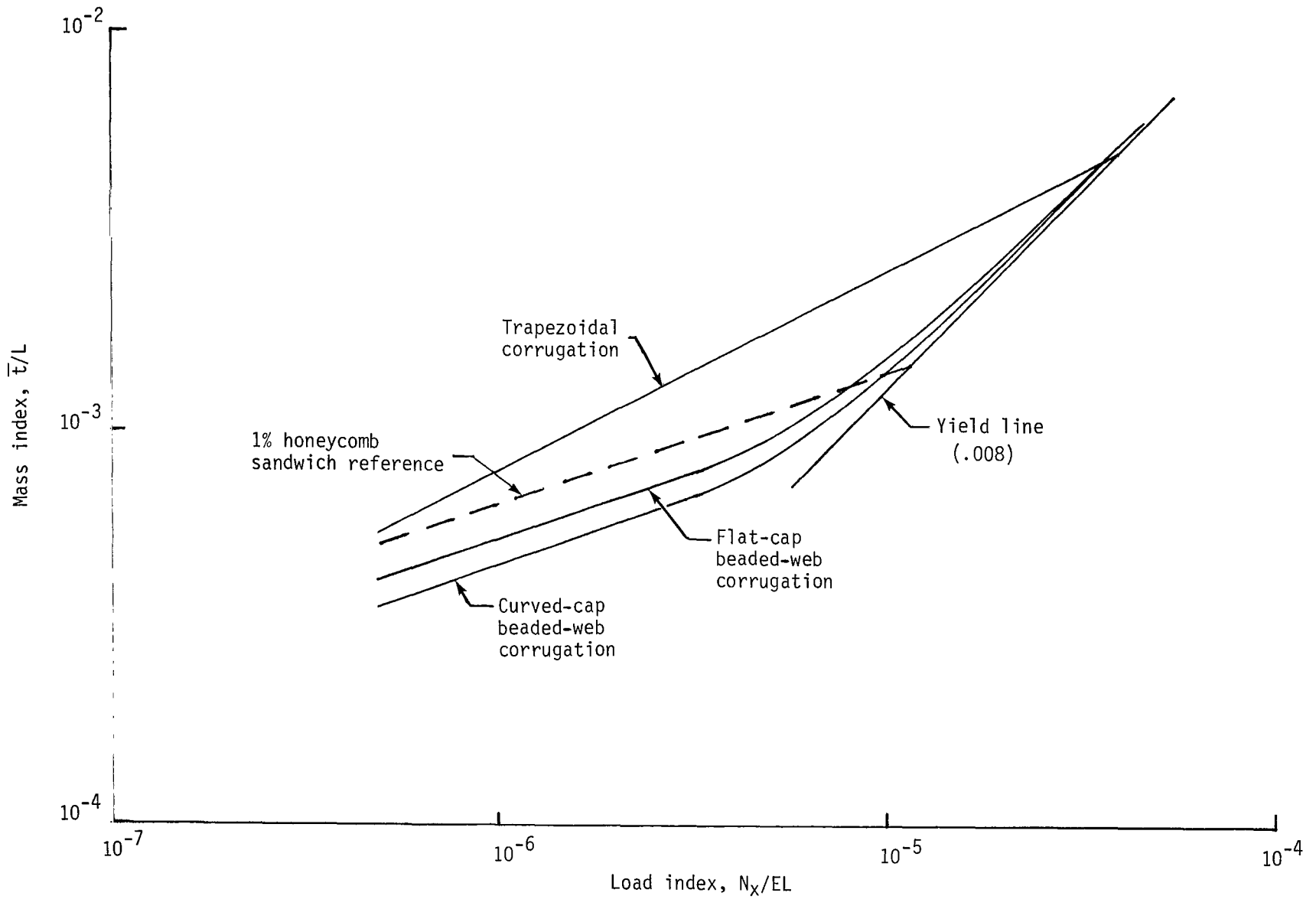
Figure 6.- Efficiency comparison for curved-cap beaded-web corrugation and flat-cap and trapezoidal corrugations.

$$\frac{\varepsilon}{k_4} = \left(\frac{t_f}{b_f}\right)^2 \left\{\frac{1}{2} + \sqrt{\frac{1}{4} + \frac{192(1 - \nu^2)n^2}{\pi^4\left[1 + 4n^2\left(\frac{t_f}{b_f}\right)^2\right]^2}}\right\}$$
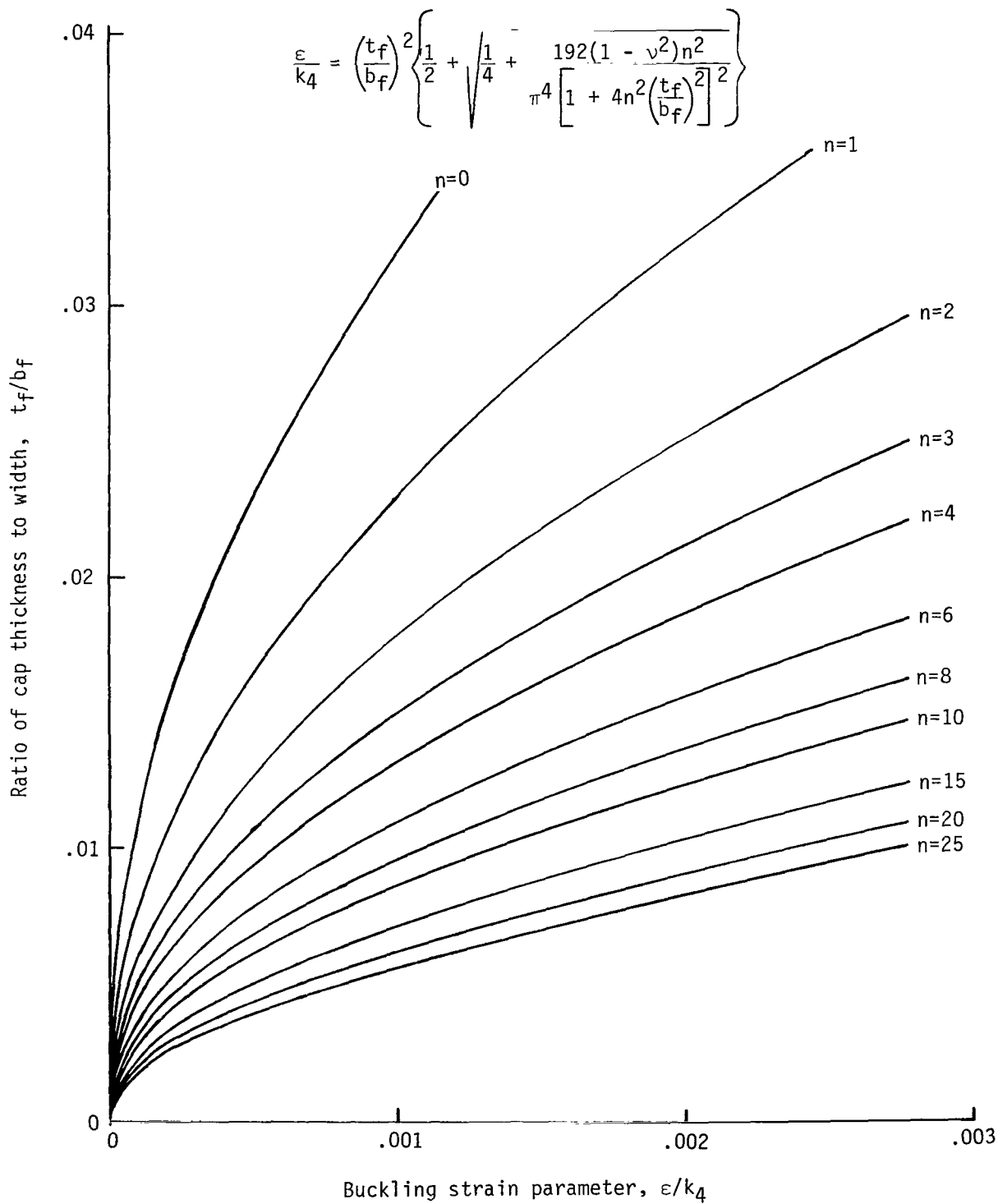
Figure 7.- Variation of ratio of cap thickness to width with local buckling strain for curved caps.
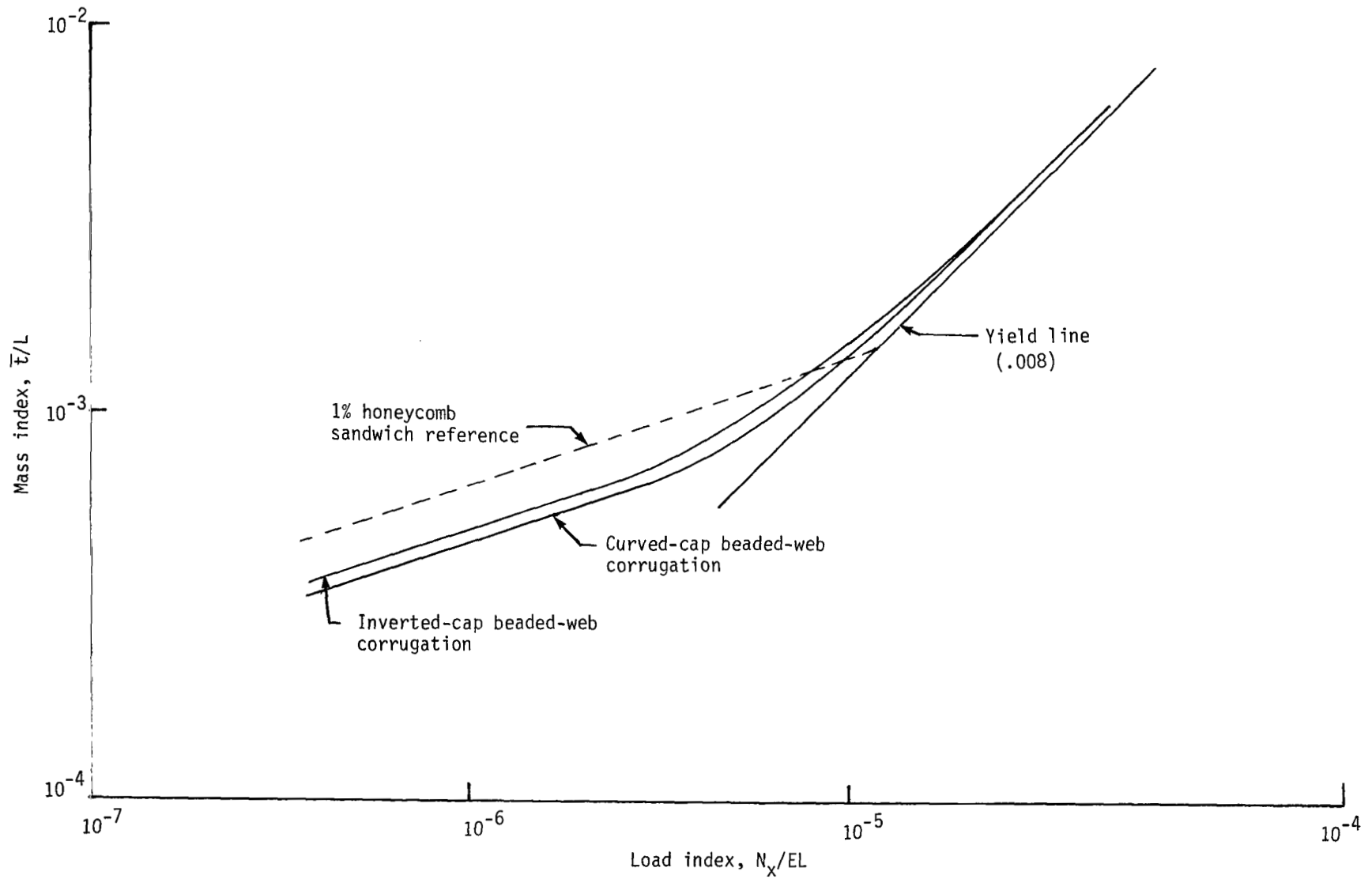
Figure 8.- Structural efficiency comparison for curved-cap beaded-web corrugation
and inverted-cap corrugation.
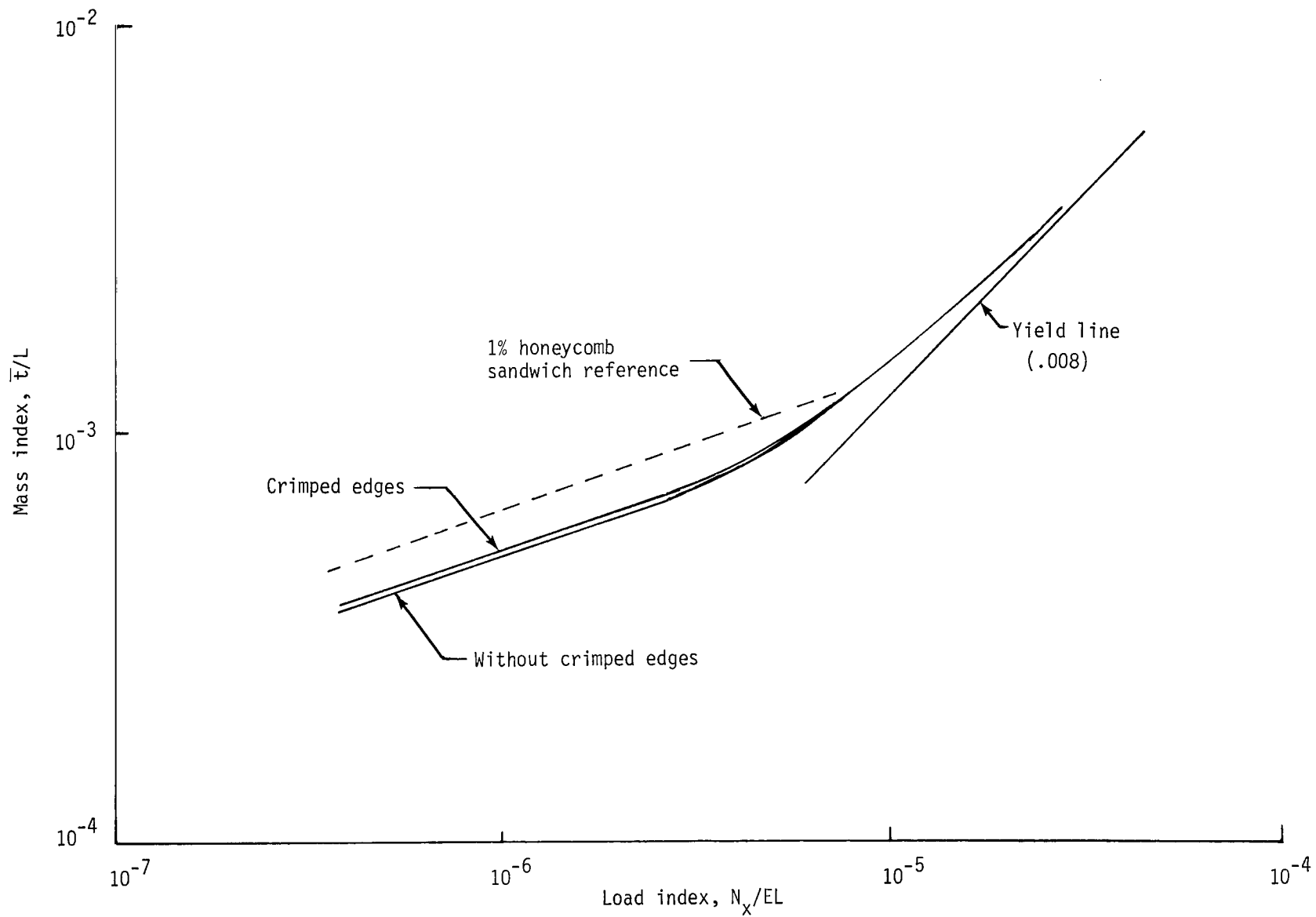
Figure 9.- Structural efficiency comparison of curved-cap beaded-web corrugation with and without crimped edges.
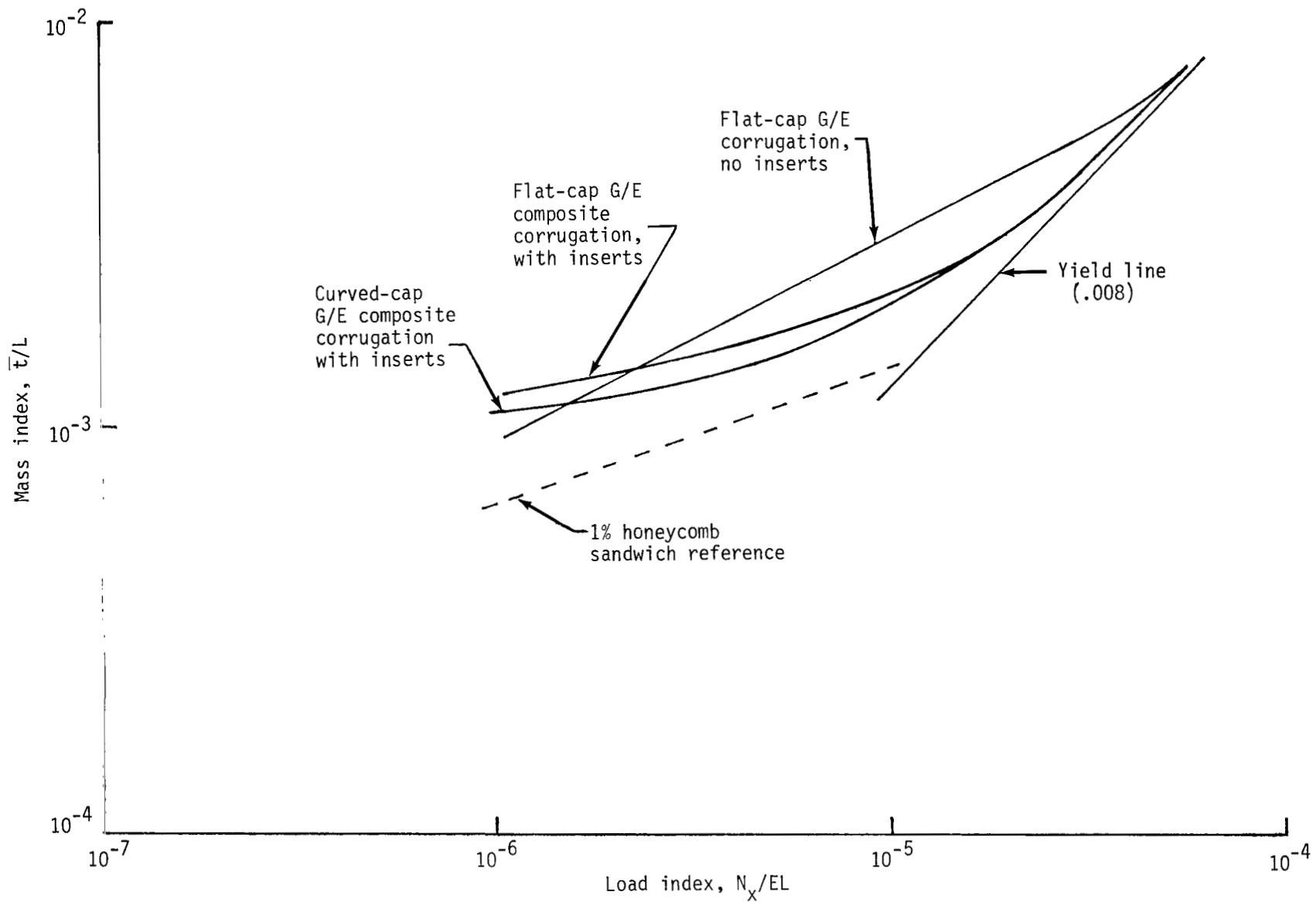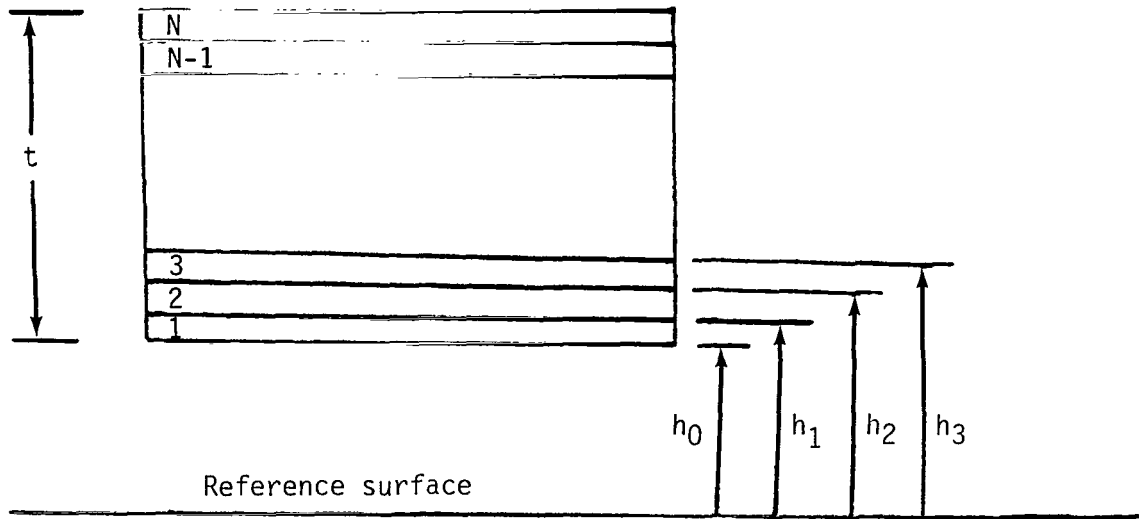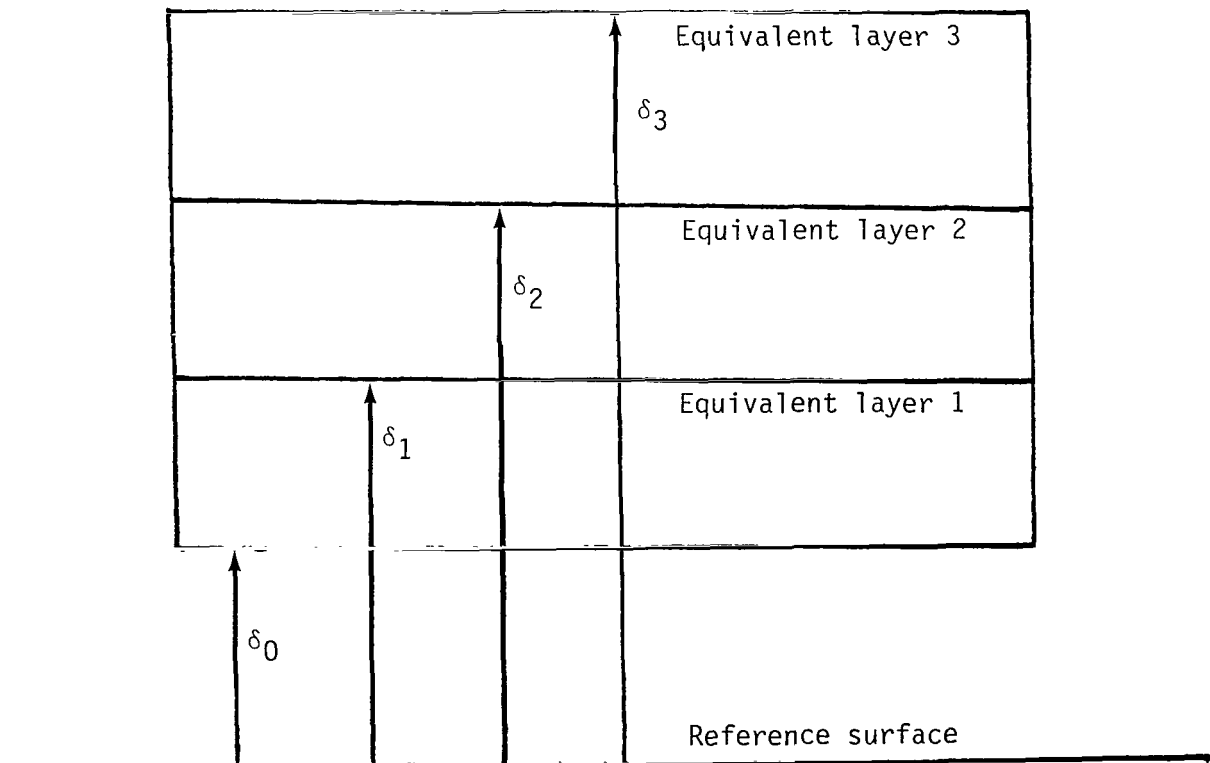
Figure 10.— Structural efficiency comparison of curved-cap graphite/epoxy (G/E) composite corrugation and flat-cap graphite/epoxy composite corrugation.

(a) Laminate nomenclature for general layup configuration.

(b) Three-layer equivalent laminate nomenclature.

Figure 11.- Nomenclature used for defining laminate cross section.

23

1. Report No. NASA TP-2272	2. Government Accession No.	3. Recipient's Catalog No.
4. Title and Subtitle STRUCTURAL EFFICIENCY STUDIES OF CORRUGATED COMPRESSION PANELS WITH CURVED CAPS AND BEADED WEBS		5. Report Date February 1984
		6. Performing Organization Code 505-33-53-11
7. Author(s) Randall C. Davis, Charles T. Mills, R. Prabhakaran, and L. Robert Jackson		8. Performing Organization Report No. L-15703
		10. Work Unit No.
9. Performing Organization Name and Address NASA Langley Research Center Hampton, VA 23665		11. Contract or Grant No.
		13. Type of Report and Period Covered Technical Paper
12. Sponsoring Agency Name and Address National Aeronautics and Space Administration Washington, DC 20546		
		14. Sponsoring Agency Code

15. Supplementary Notes

Randall C. Davis and L. Robert Jackson: Langley Research Center, Hampton, Virginia.
Charles T. Mills and R. Prabhakaran: Old Dominion University, Norfolk, Virginia.

16. Abstract

Curved cross-sectional elements are employed in new structural concepts for minimum-mass compression panels. Corrugated panel concepts with curved caps and beaded webs are optimized by using a nonlinear mathematical programming procedure and a rigorous buckling analysis. These new panel geometries are shown to have superior structural efficiencies compared with known concepts published in the literature. Fabrication of these efficient corrugation concepts has become possible by advances made in the art of superplastically forming of metals. Results of the mass optimization studies of the concepts are presented as structural efficiency charts for axial compression.

17. Key Words (Suggested by Author(s)) Structural efficiency Corrugations Superplastically forming Minimum mass Composites Compression panels Buckling strength	18. Distribution Statement Unclassified – Unlimited Subject Category 39

19. Security Classif. (of this report) Unclassified	20. Security Classif. (of this page) Unclassified	21. No. of Pages 24	22. Price A02

National Aeronautics and
Space Administration

Washington, D.C.
20546

Official Business
Penalty for Private Use, $300

U.S.MAIL

NASA